Properties and structure of Faraday rotating glasses for magneto optical current transducer

BOLETIN DE LA SOCIEDAD ESPAÑOLA DE
Cerámica y Vidrio
www.elsevier.es/bsecv

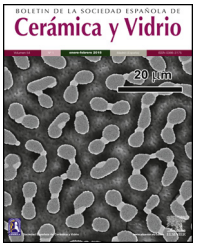

Properties and structure of Faraday rotating glasses for magneto optical current transducer

Qiuling Chen[a,*], Qiuhua Ma[a], Hui Wang[b], Qingwei Wang[a], Yinlei Hao[c], Qiuping Chen[b]

[a] School of Material Sciences & Engineering, Henan University of Technology, Zhengzhou 450007, Henan, China
[b] Department of Applied Science and Technology, Politecnico di Torino, Corso Duca degli Abruzzi, 24, Torino 10129, Italy
[c] Department of Information Science and Electronic Engineering, Zhejiang University, Hangzhou, China

ARTICLE INFO

Article history:
Received 22 February 2016
Accepted 20 July 2016
Available online 8 August 2016

Keywords:
Heavy metal oxides glass
Faraday effect
Verdet constant

ABSTRACT

High heavy metal oxides (60–100 mol.%) ternary PbO–Bi_2O_3–B_2O_3 (PBB) glasses were fabricated and characterized. Using a homemade single lightway DC magnetic setup, Verdet constants of PBB glasses were measured to be 0.0923–0.1664 min/G cm at 633 nm wavelengths. Glasses with substitution of PbO by Bi_2O_3 were studied in terms of their Faraday effects. PbO–Bi_2O_3–B_2O_3 = 50–40–10 mol.% exhibited good thermal stability, high Verdet constant (0.1503 min/G cm) and good figure of merit (0.071). Based on this glass, a magneto optical current sensor prototype was constructed and its sensitivity at different currents was evaluated to be 8.31 nW/A.

Propiedades y estructura de los vidrios rotadores de Faraday del transductor de corriente magneto-óptico

Palabras clave:
Vidrio de óxidos de metales pesados
Efecto Faraday
Constante de Verdet

RESUMEN

Se fabricaron y se calificaron vidrios ternarios PbO-Bi_2O_3-B_2O_3 (PBB) de óxidos metálicos muy pesados (60-100 mol%). Con una sencilla y simple instalación magnética de corriente continua se midieron las constantes de Verdet de los vidrios de PBB de 0,0923-0,1664 min/G cm, a longitudes de onda de 633 nm. Se estudiaron los efectos Faraday en los vidrios con una sustitución de PbO por Bi_2O_3. PbO-Bi_2O_3-B_2O_3 = 50-40-10 mol% mostró una buena estabilidad térmica, una constante de Verdet elevada (0,1503 min/G cm) y un buen factor de mérito (0,071). Sobre la base de este vidrio se construyó un prototipo de sensor de corriente magneto-óptico y se evaluó su sensibilidad a diferentes corrientes para llegar a 8,31 nW/A.

* *Corresponding author.*
E-mail address: qiuling.chen@polito.it (Q. Chen).
http://dx.doi.org/10.1016/j.bsecv.2016.07.002

Introduction

Magneto-optical current transducers (MOCT) based on Faraday effect have been developed worldwide as alternative to conventional optical ones [1] because MOCTs are compact and lightweight, immune to electromagnetic noise, and they offer a wide measurement range and long distance signal transmission [2]. Based on principle of Faraday effect, high rotation material is fundamental for getting a high sensitivity. Currently used high rotation materials are crystals (Bi:YIG etc.), or garnets and rare earth doped paramagnetic glasses, However, these expensive materials have limited magneto optical response to currents due to their temperature-dependent property [3–5].

Unlike its paramagnetic counterpart, diamagnetic heavy metal oxide (HMO) glasses, such as Bi_2O_3 and PbO, due to their mass and high polarizability of ions Pb^{2+} and Bi^{3+}, are appealing for magneto optical sensors because of their temperature-independent Faraday effect, small phonon energy, large refractive index and low-melting properties [6].

Bi_2O_3-based glasses have attracted a great deal of research interest because of their high optical transmission into the far-infrared region (in the range 0.5–8.7 mm), non-linear optical behavior and efficient luminescent applications in lasers. The modifier oxide, PbO, when added to bismuth borate glasses, the glasses are expected to become highly stable against devitrification and chemically inert [7] since PbO, in contrast with the conventional alkali/alkaline earth oxide/halide modifiers, form the stable glasses due to its dual role—modifier (with PbO_6 structural units) and glass network former in both covalent and ionic bonding with $PbO_4/2$ pyramidal units connected in puckered layers or frame structure [7,8]. Although Bi_2O_3 and PbO do not form glass by their own, they modify a vitreous network to form glass when they were combined with B_2O_3 [9,10] which is a good glass forming oxide for technological applications.

Most studies on PbO, Bi_2O_3 based glasses are multicomponents. Reports on PBB glass doped with other elements, such as SiO_2, Er/Yb [11–13], Tm, Tb/Ce [14], V_2O_5 Tb/Dy [15] and TiO_2 [16] etc. can be found for laser, luminescence [17], photosensitivity, non-linearity and dielectric dispersion applications [18]. Magneto-optical properties of multicomponents $PbO–Bi_2O_3$ doped with GeO_2 [6,19], ferrimagnetic FeO [20]/Fe_3O_4 [21], TeO_2 [22], CdO/MnO and Ga_2O_3 [23] etc. were reported. Spectral study of binary glass system $PbO–B_2O_3$, $Bi_2O_3–B_2O_3$ and $PbO–Bi_2O_3$ [24] can be found as gamma-radiation shielding materials [25] and ion conductor.

Till now, two literature reported on Raman spectra/optical [26] and dispersion [27] property of ternary $PbO–Bi_2O_3–B_2O_3$ for non-linear and optical coating application, respectively. The magneto-optical properties of ternary PBB glass were investigated by a new Faraday measurement method by this group [28]. Further study such as doping Fe_3O_4 nanoparticles [21] and GeO_2 [29] into ternary PBB glass were continued. Detailed study on this system is of big interests because this system has many potential applications in photonics and magneto-optical fields. The main challenge is the synthesis of PBB glass, because it is known that Bi_2O_3 and PbO are not traditional glass former, but Bi^{3+} and Pb^{2+} are highly polarizable ions and the asymmetry of their polyhedral inhibits the crystallization processes in the melts in PBB system [14]. Also the processing conditions of the HMO glasses influence the optical quality and color of samples [30]. In addition, the steep viscosity–temperature relationship and high thermal expansion in high lead/bismuth glasses [31] also hinder the study on ternary PBB glass.

Based on our previous study [21,22,28–30] on the processing condition and Faraday rotation measurement method, in this article, we directed a more systematically study on PBB glasses with a high HMO concentrations ranging from 60% to 90% in mol., and focus on their Faraday rotation in magneto optical sensors application. The aim of this study is to find a PBB with the best thermal and magneto optical performance for MOCT prototype construction. The sensitivity of MOCT was evaluated under different currents to verify the Faraday performance of selected glass.

Experiment

Glasses of nominal compositions were fabricated by melt-quenching method. Optical grade reagents (Aldrich, purity 99.9%) PbO, B_2O_3 and Bi_2O_3 were weighted and mixed in Al_2O_3 crucibles at melting temperatures ranging from 900 °C to 1100 °C for 1 h and were cast on a 200 °C preheated brass plate. The cast bulk glasses were annealed for 2 h at temperature ranging from 300 °C to 350 °C at 1 °C/min heating/cooling rate. The fabricated glasses were bubble-free, highly homogeneous and transparent with a yellow color. The sample with the optimum composition, assuring the best glass forming and physical properties, was chosen as sensing element for MOCT. The annealed glasses were cut into parallel slabs with a thickness of 2.5 mm and optically polished using a polishing instrument (λ – Logitech PM5).

Glass transition temperature (T_g) and crystallization temperature (T_x) were determined by differential scanning calorimetry (Perkin-Elmer DSC7), under N_2 atmosphere at a heating rate of 10 °C/min. The density was calculated at room temperature following the Archimedes' principle using water as immersion liquid. The refractive index (n) was measured under different wavelengths by the prism coupling method using Metricon 2010. The UV absorption spectra were recorded in the wavelength range of 200–800 nm by means of a UV-VIS spectrophotometer (Varian Cary 500) using optically polished samples with a thickness of 2.5 mm. Using samples thickness, the absorption coefficient can be calculated by equation: $\alpha = \log(I_0/I)/z = A/z$, where α is the absorption coefficient, A is the absorbance obtained from UV spectra, z is the sample thickness (z = 2.5 mm). The cut off is defined as the wavelength at which light ceases to propagate in the medium, it is normally calculated as the one at which the transmission decreases to 50% of its maximum. Fourier transforms infrared spectra (FT-IR) measurements from 1500 to 4000 cm^{-1} wave number were carried out using a Varian Cary 500 spectrophotometer.

The Verdet constants of glasses were measured using a home-made optical bench as shown in Fig. 1. A He–Ne laser, emitting 1.8 mW in a linearly polarized laser beam about 1 mm in diameter, was focused on the glass using a 10× microscope

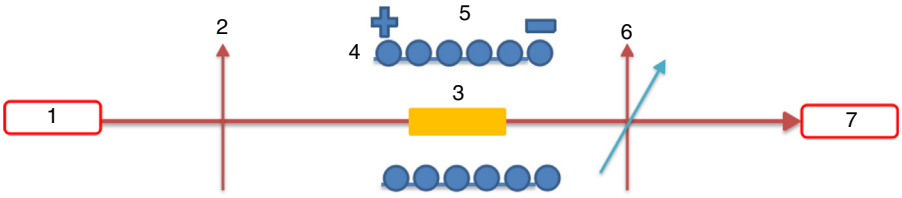

Fig. 1 – Schematical setup for Verdet constant measurement of PBB glass, 1: He–Ne laser, 2: polarizer, 3: MO glass, 4: solenoid, 5: current supplier, 6: analyzer, and 7: detector.

objective with NA = 0.28, resulting in a launching efficiency of 29%. The polarization extinction ratio of the laser beam was measured to be better than 1:5000. Glass samples were mounted in a solenoid which wrapped with a copper electrical wire, 2 mm in diameter, coiled into 220 turns around a 19 cm long a polymeric tube with a radius of 11.5 mm. The overall outer radius of the electrical coil was 17 mm.

As demonstrated in Fig. 1, the polarized beam propagates through the glass and then passes through an analyzer, which was mounted on a rotational stage graduated with a precision of 3×10^{-4} rad. The power of the output beam was then measured using a photo detector (Ophir PD300) having a dynamic range of 30 dB down to a power level of 0.02 nW. A pure silica (with a known Verdet constant in literature [32,33]) is used as the reference for the sake of precise.

A MOCT prototype was constructed using PBB glass as sensing element as shown in Fig. 2. The setup consists of two linear polarizers, PBB glass, the conductor (Ø = 34 mm), laser and photodiode detector. The sensing head was fixed within the conductor. A DC current supplier was connected in series to the conductor for current supplying. The response signal was collected by photo-detector through which the signal can be converted to electric intensity. The sensitivity to current can be calculated and expressed by output intensity response to applied current [29].

Results and discussion

Glass forming

All of the obtained glasses are transparent, free of bubbles, yellow in color with good quality. For the aim of investigate the influence of PbO and Bi_2O_3 to the glass forming ability, 6 binary glasses PBB01–PBB06 were fabricated as comparison to ternary. From Table 1, it can be seen that binary PbO and Bi_2O_3 could not form glass (i.e. PBB01, PBB02) by themselves, PbO had a wider glass formation ability with B_2O_3 than Bi_2O_3 at same concentration (PBB03 and PBB04 are glasses, but PBB05 and PBB06 could not form glass). Substitution of Bi_2O_3 (or PbO) with PbO(or Bi_2O_3) in binary PbO–B_2O_3 and Bi_2O_3–B_2O_3 systems [11] resulted much stable ternary PBB glasses (PBB12–PBB17 and PBB21–PBB29). This good glass forming ability of ternary PBB came from contribution from B^{3+} and from the high polarizability of the Pb^{2+} and Bi^{3+} ions, which have outer shells of eighteen electrons.

Probable reasons for glass forming and crystalline of binary and ternary PBB systems are addressed from different aspects.

1. From the structure: Fig. 3 illustrates the structure of PbO, it can be seen that one Pb ion is surrounded by eight oxygen ions, in which four O^{2-} are far from Pb (0.429 nm), while the other four O^{2-} are closer (0.23 nm), thus the coordination is asymmetric. The inert electrons outside the Pb ion are rejected by the nearest oxygen which push the Pb ions to the other oxygen side, so it can be assumed losing two electrons and considered as a Pb^{4+} nucleus. While on the other hand, the other four O^{2-} which are far away from the Pb, can be assumed receiving two electrons and considered as Pb^0. Since the Pb locates at the top of PbO_4 pyramidal unit. So the Pb^{2+} in the pyramidal unit can be considered as $-1/2Pb^{4+}-1/2Pb^0-$ structure. The $1/2Pb^0$ termed as metal bridge decreases glass forming ability.
2. From the crystalline chemistry: The number of unpaired electrons in orbit for Pb, Bi and O elements are 2, 3 and 2, respectively, so from the point of view of the possibility of

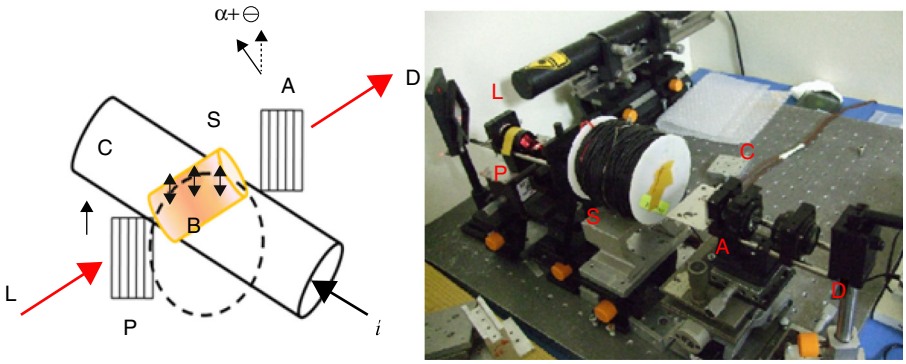

Fig. 2 – Schematic and actual setup for PBB glass based MOCT. L: laser, P: polarizer, C: conductor with current, S: solenoids with sample inside, A: analyzer, and D: detector.

Table 1 – Composition (mol.%) of the prepared PBB glasses and glass forming appearance.

Code	PbO	Bi_2O_3	B_2O_3	Glass-forming
PBB01	90	10		Glass[a,b]
PBB02	80	20		Ceramic
PBB03	90		10	Glass[a,b]
PBB04	80		20	Glass[a]
PBB05		90	10	Crystalline
PBB06		80	20	Crystalline
PBB10	80	10	10	Ceramic
PBB11	70	20	10	Glass/crys.[b]
PBB12	60	30	10	Glass
PBB13	50	40	10	Glass
PBB14	45	45	10	Glass
PBB15	40	50	10	Glass
PBB16	35	55	10	Glass
PBB17	30	60	10	Glass[a]
PBB18	20	70	10	Slight crystalline[b]
PBB19	10	80	10	Crystalline
PBB21	70	10	20	Glass
PBB22	65	15	20	Glass
PBB23	55	25	20	Glass
PBB24	50	30	20	Glass
PBB25	45	35	20	Glass
PBB26	35	45	20	Glass
PBB27	25	55	20	Glass
PBB28	15	65	20	Glass
PBB29	10	70	20	Glass[a]
PBB31	35	35	30	Glass/little broken[a,b]
PBB41	25	35	40	Broken to pieces[a,b]

[a] Mold needs to be preheated to 200–250 °C during casting.
[b] Annealing should be done immediately after casting.

forming bond, Pb and O, Bi and O can form covalent bonds by sharing electrons. Pb, Bi and O atoms bond, in the molten state, they exist as Pb^{2+}, Bi^{3+} and O^{2-}. During cooling, due to electrostatic force these ions accumulate together, and ion crystals are formed. Therefore, it is difficult to form glass for single oxide and binary oxides of PbO and Bi_2O_3.

3. From the point of dynamics, crystallines mainly depends on the formation of nucleus and the growth of nucleus into crystals. Because the viscosity of molten PbO and Bi_2O_3 is very small, so the active energy for Pb^{2+}, Bi^{3+} and O^{2-} diffusion is also small, the nucleus is easy to grow into bigger crystals.

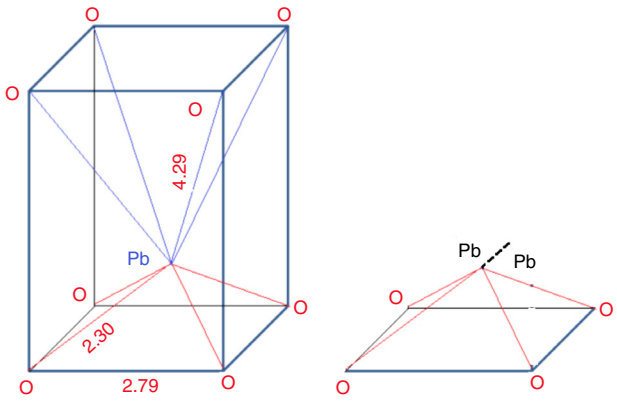

Fig. 3 – Schematic structure of PbO.

4. While for ternary PBB system, due to B—O bond strength is very big (498 kJ/mol), the introduced B_2O_3 exist in the form of isolated layered triangular $[BO_3]$ or tetrahedral $[BO_4]$ which surround the accumulated Pb^{2+}, Bi^{3+} and O^{2-} and therefore prevent their growth. On the other hand, $[BO_3]$ or tetrahedral $[BO_4]$ occupy certain space and inhibit the transfer or diffusion of Pb^{2+}, Bi^{3+} and O^{2-}, making the Pb^{2+}, Bi^{3+} and O^{2-} outside the $[BO_4]$ surrounding cannot enter and accumulate with ions inside, and finally stop the formation of crystals and easy glass-forming.

A ternary diagram was plotted according to glasses compositions in this study, also a theoretically diagram for ternary glass consisting one F (former) and two high polarized heavy metal oxides modifier (M) was presented as a reference. From Fig. 4, it can be seen that PbO and Bi_2O_3 cannot form binary system, while it is possible to form binary PbO–B_2O_3 and Bi_2O_3–B_2O_3 system. Initially, a molten glass network based on PbO and B_2O_3 was formed firstly, with the incorporation of Bi_2O_3 into the network, more free oxygen was introduced, and the melting temperature decreased. An equilibrium was reached until the lowest co-melting point appear. And a continuous ternary glass forming range (11′22′) formed. Due to the double rule of PbO, the lowest co-melting point should be close to PbO, and the binary PbO–B_2O_3 has a wider forming glass range (22′) than Bi_2O_3–B_2O_3 system (11′). The experimental PBB glass forming diagram agreed very well with theoretical one.

For PBB glasses with HMO of 90%, when Bi_2O_3 >60% or Bi_2O_3 <30%, the melts form ceramic or crystalline, not glass. This proved that Bi_2O_3 had a substantial effect on the process of glass crystallization. When Bi_2O_3 >70%, PBB18 began to crystalline, when Bi_2O_3 >80%, PBB19 became ceramic.

From Table 1 it can be seen that glasses with HMO = 80% had a bigger glass forming ability than glasses with HMO = 90%. This is due to the increase of B_2O_3. The role of B_2O_3 in glass matrix is enhancing the glass structure by decreasing the crystalline trends. When HMO = 80%, PbO and Bi_2O_3 had a bigger glass forming range from 10 to 70%. But when B_2O_3 = 30%, PBB31 exhibited poor mechanical property while when B_2O_3 = 40% (PBB41), the melts broken to pieces during casting which proved a very poor mechanical property. These phenomena can be explained by B_2O_3 performance. It is well known that, with the increase of B_2O_3, the introducing of modifiers like PbO, Bi_2O_3, will convert the sp2 planar BO_3 into more stable sp3 tetrahedral BO_4 units in addition to non-bridging oxygens as illustrated in Fig. 5.

According to theoretical relationship between $[BO_4]$ with oxides, the number of $[BO_4]$ increase sharply and almost linearly (except the Li_2O_2) with oxides content in glass. Considering the high oxide content (70–90%) in this study, the B_2O_3 in glass present mainly as $[BO_4]$ unit.

Due to structural (shape) mismatch of $[BO_3]$ and $[PbO_4]$, it is hard to form homogeneous and dissoluble molten which will induce the phase separation during cooling. Oxides transfer the B_2O_3 structure through offering free oxygen, and change the layered triangle $[BO_3]$ to frame tetrahedron $[BO_4]$ which can be easily dissolve into the $[PbO_4]$ and form homogeneous glassy network, because in layered triangle $[BO_3]$ structure, even though the B—O bond strength is big (498 kJ/mol), the

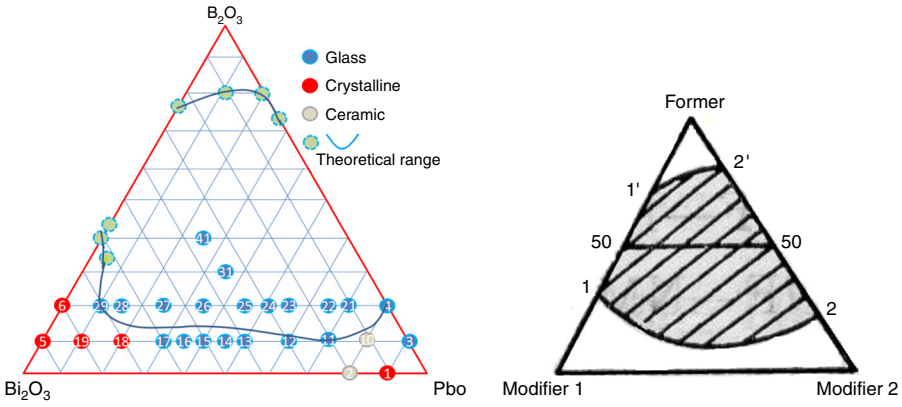

Fig. 4 – Experimental and theoretical diagram for PBB glass.

energy between layers are mainly Van Edward force which is very weak, the layered structure is unstable and can be easily broken. While the frame structure [BO_4] is more stable, and highly connectivity to [PbO_4]. On the other hand, considering the glasses fabricated are transparent and good quality, it can be deduced that B_2O_3 present in glass mainly in the form of [BO_4], not [BO_3].

Simulation of PBB system employed Amorphous cell program in Materials Studio simulation software was carried out to prove the assumption. The simulated two PBB systems are based on: 68PbO–24Bi_2O_3–8B_2O_3 and 61PbO–21Bi_2O_3–18B_2O_3 in mol percent, finally using DMOL3 modulus to optimize the structure (Fig. 6).

In 68PbO–24Bi_2O_3–8B_2O_3 glass, the B_2O_3, as a glass former, exists as [BO_4] which is highly connected with the [PbO_4] network, while [BiO_6] as a modifier. In 61PbO–21Bi_2O_3–18B_2O_3 glass, the B_2O_3 exist both as [BO_4] and [BO_3], it can be observed that the [BO_4] unit connected with [PbO_4] as network former, while the excessive B_2O_3 is isolated by the network in the form of [BO_3].

In the case of B_2O_3 content is beyond a certain limit (e.g. 30% in mol.), the excessive B_2O_3 transfer the form of [BO_4] into [BO_3] due to the famous boron anomaly. It can be deduced that, with the increase of [BO_3] unit, more and more [BO_4] units were transferred to [BO_3], and PBB glass structure become more and more loose, so accordingly the glass forming ability and glass properties degraded greatly, until no possibility to form PBB glass (e.g. glass with 40% B_2O_3).

Thermal property

Table 2 gives properties of PBB glasses.

The T_g gives information on both the strength of interatomic bonds and the glass network connectivity [21], from Table 2, one can observe that T_g always decreases when increasing of PbO + Bi_2O_3 content as a whole. This is because the addition of PbO + Bi_2O_3 weakened the bond between each atom in the network and increased the number of non bridging oxygens, especially in O—B linkages. Continuous substitution of B_2O_3 by PbO + Bi_2O_3 leaded to a continue decrease in T_g. The substitution of stronger B—O bonds (498 kJ/mol) by weaker Pb—O bonds (305 kJ/mol) and Bi—O induces the increase of non bridging oxygen atoms number and a bigger tendency to form BO_3 units. As a consequence, the network is soften and weaken with lower thermal stability $\Delta T = T_g - T_x$.

In addition, Pb^{2+} ions and Bi^{3+} had lower electrical field intensity (0.27 and 0.23) than B^{3+} ions (>1.4) [34], so PbO

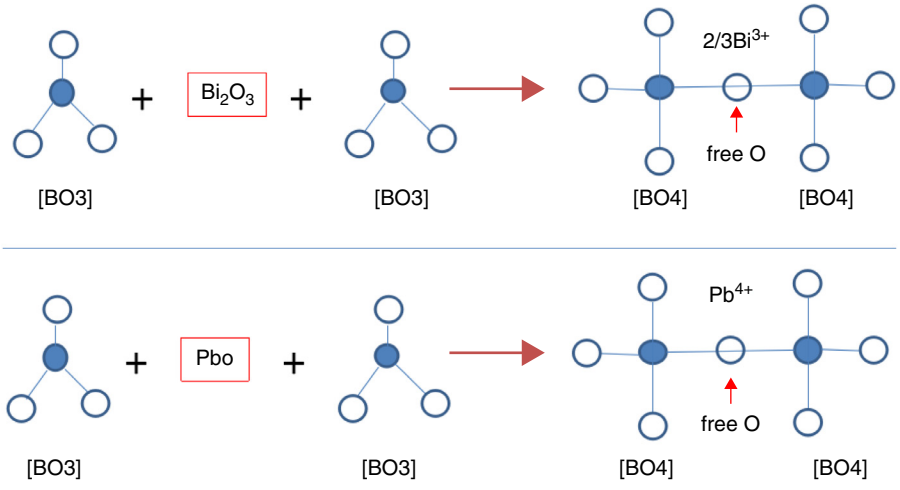

Fig. 5 – Evolution of [BO_3] to [BO_4] in PBB glass.

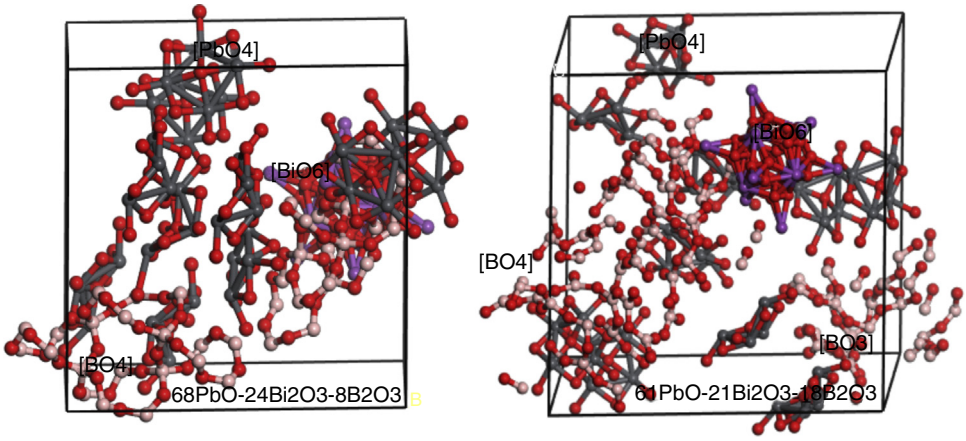

Fig. 6 – Simulation of PBB glass structure as a function of B_2O_3 content.

Table 2 – Composition (mol.%), glass transition temperature (T_g), crystalline temperature (T_x), density (ρ), cutoff wavelength (λ) and Verdet constant (V), refractive index (n), optical absorption (α) at 633 nm of glasses.

Glass code	V (min/G cm)	ΔT (°C) ($T_x - T_g$)	T_g (±1 °C)	T_x (±1 °C)	n ±0.01	ρ (kg/m³)	a (cm^{-1}) (×10^{-5})	Q	λ (nm) ±1
PBB12	0.1373	80	317	397	2.26027	8.29	2.3241	0.059	464
PBB13	0.1503	89	289	378	2.27451	8.31	2.15	0.071	474
PBB14	0.1475	62	327	389	2.32241	8.36	2.5610	0.053	469
PBB15	0.1492	56	330	386	2.33251	8.39	2.5640	0.051	471
PBB16	0.1512	53	332	385	2.33620	8.42	2.5613	0.057	473
PBB17	0.1518	41	330	371	2.33731	8.54	2.5662	0.051	475
PBB21	0.1042	94	303	397	2.20711	8.58	2.2136	0.041	441
PBB22	0.1089	87	305	392	2.1344	7.99	2.27	0.048	449
PBB23	0.1109	84	304	388	2.16473	8.03	1.9291	0.053	450
PBB24	0.1194	75	303	378	2.1993	8.11	2.1631	0.048	452
PBB25	0.1252	79	306	385	2.2056	8.16	1.9982	0.067	454
PBB26	0.1264	98	302	400	2.2066	8.25	2.3211	0.056	455
PBB27	0.1299	73	310	383	2.1577	8.26	2.3145	0.059	457
PBB28	0.1329	68	311	379	2.1582	8.31	2.3201	0.059	459
PBB29	0.1351	62	309	371	2.1601	8.37	2.3984	0.037	460

and Bi_2O_3 exhibited high polarisability, the high polarisability explains why the T_g shifted toward lower temperature [35].

Fig. 7 shows the T_g, T_x changes with the PbO in different HMO contents. Based on same HMO content, substituting of PbO with Bi_2O_3 leads to a decrease in the molar volume and decrease in T_x because the network starts to be cross-linked due to BO_3 (planar trigonal units) to BO_4 (tetrahedral units) conversion [36]. This also could be ascribed to the introduction of more free oxygen, as a polarizable component into the glass structure when substituting of PbO with Bi_2O_3 [37,38]. Additionally, introducing more Bi^{3+} cations, as a glass modifier, would cause structural complexity which could ease

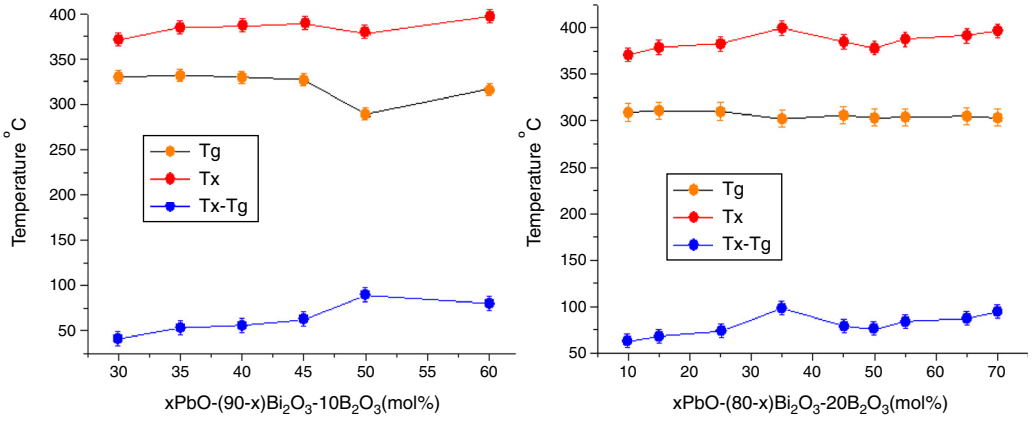

Fig. 7 – Relationship between PbO content with T_g and T_x for PBB glasses.

the divetrification [39]. So increasing of Bi_2O_3 at the cost of reducing PbO induced poor thermal stability of glasses. While on the contrary, B_2O_3 helps to increase the thermal stability within certain limit. For example, the average ΔT of glasses PBB12–PBB17 was lower than that of PBB21–29. Among all glasses, the glass with composition of $35PbO–45Bi_2O_3–20B_2O_3$ in mol.% showed the highest ΔT.

Refractive index

Refractive index of glass is sensitive to network structural changes [40], so it is generally influenced by the bond polarizabilities of its constituents. In the case of conventional glasses, it has been observed that both the linear and nonlinear refractive indices increase with the concentration of non-bridging oxygen bonds that are induced by the addition of network modifiers. However, this is not the case for glasses with a significant fraction of heavy metal cations with ns2 electron pairs (Pb^{2+}, Bi^{3+}). In this case, the concentration of heavy metal cations, and in particular their high polarizability and big atomic mass, are main factors determining refractive index values.

From Table 2, the refractive indices of PBB12–PBB17 as a whole are higher than that of PBB21–PBB29, and they increased with the Bi_2O_3 content at the cost of PbO. This is because with the incorporation of Pb^{2+} ($r = 0.132$ nm, $\alpha = 1.315$ nm^3) and Bi^{3+} ($r = 0.103$ nm, $\alpha = 1.508$ nm^3), when light passes through the glass, more energy was required to distort electron cloud of Pb^{2+} and Bi^{3+}, so a great part of the energy is converted into the vibration energy outside the nucleus field, and the propagation speed is greatly influenced, eventually leading to the improvement of refractive index [11].

Beside the polarizability, the phenomenon of 'Boron anomaly' also influences the refractive index. It is related to the boron ion co-ordination number changes from 3 to 4, when PbO or Bi_2O_3 are introduced [19,21,28], that is why even at the same HMO contents, the refractive index varied when PbO played different roles.

Optical absorption and cutoff wavelength

As addressed in previous section, when light pass the glass, a great part of the light energy is converted into the vibration energy outside the nucleus field for electron cloud distortion, so the optical absorption inside the glass would increase. From Table 2, the optical absorption of glasses with HMO = 90% were higher than glasses with HMO = 80%. Another reason for the absorption is the color changed at different compositions; for example, the color of glass with 90% HMO were dark yellow, while colors for glasses with HMO = 80% were light yellow. Even based on same HMO content, PbO-rich-glasses were yellow, while Bi_2O_3-rich-glasses were brown, and the brownish color intensified on prolonged stirring of the melts [18]. Fig. 8 shows the UV–vis spectra and cutoff of PBB glasses.

It can be seen that all glasses exhibited a steep cutoff and this makes them an appealing candidate in optical switches [41] and shielding applications. In addition, the cutoff shifted to longer wavelengths with the increase of $PbO + Bi_2O_3$ contents. For the same HMO content, cutoff of glasses shifted to shorter wavelength with the substitution of Bi_2O_3 with PbO

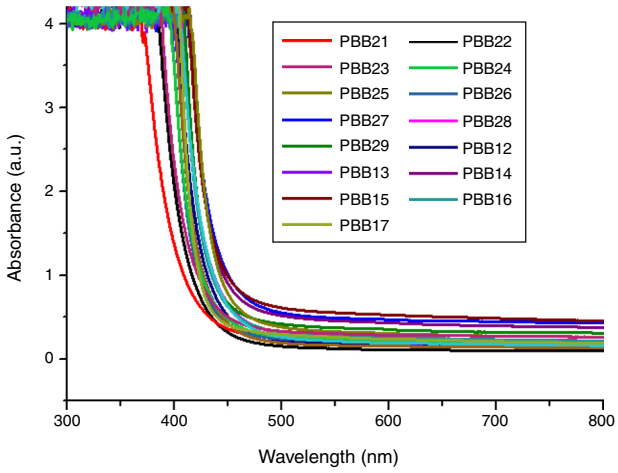

Fig. 8 – UV-vis spectra for PBB glasses.

as shown in Fig. 9. There are 3 reasons for the cutoff shifts with different compositions:

1. The increase in molecular mass of oxides can induce the red-shift of glass cutoff which agreed well with [42]. From Table 1, when HMO = 90%, glass PBB17 had the highest Bi_2O_3 (60%), because the molecular mass of Bi_2O_3 is 465.96 g/mol, while mol. masses for PbO and B_2O_3 are 223.2 g/mol and 69.62 g/mol respectively, and PBB17 had the biggest red-shift compared with other glasses. In these glasses, the Bi_2O_3 contributed more to the UV cutoff red-shift than PbO.
2. From the point of polarizability, the Bi_2O_3 induced more red-shift of UV cutoff than PbO [43]. Due to the fact that lead oxide offers only one atom per molecule, whereas bismuth oxide contributes two bismuth cations. Bi^{3+} cation possesses an extremely low electronic polarizability (0.002 Å^3) (while for Pb^{2+} (4.9 Å^3) and its unit field strength is very large which affecting strongly the electron charge density of the surrounding oxygen ions. So Bi^{3+} cations have a high polarizability (1.508 Å^3) [40] and small cation oxygen field strength. Therefore, glasses with more Bi_2O_3 had higher oxide ion polarizability and this induced more red-shift.
3. From the point of glass energy band gap. The shift in cutoff could also be explained by the change of band gap for different constituents in glass systems: the band gap $E_g = hc/\lambda$, where h and c are constants, λ is the cutoff wavelength. The E_g for B_2O_3 is 8 eV, E_g for PbO is 2.73 eV and E_g for Bi_2O_3 is 2.76 eV. The decrease of E_g in the glass can move the UV cutoff to longer wavelength. So the increase of HMO red-shifted the UV cutoff, at the same HMO content, PbO-rich glasses has shorter cutoff wavelength than Bi_2O_3-rich glasses.

FT-IR spectra

The FT-IR spectra of glasses recorded in the range of 1500–4000 cm^{-1} are displayed in Fig. 10. The different roles of PbO induced difference of FT-IR transmission. Normally PbO acts as a glass modifier at low content and enters the glass as Pb^{2+} ions, the Pb—O bonds strongly ionic and the cations enter the network in an interstitial manner. Every added

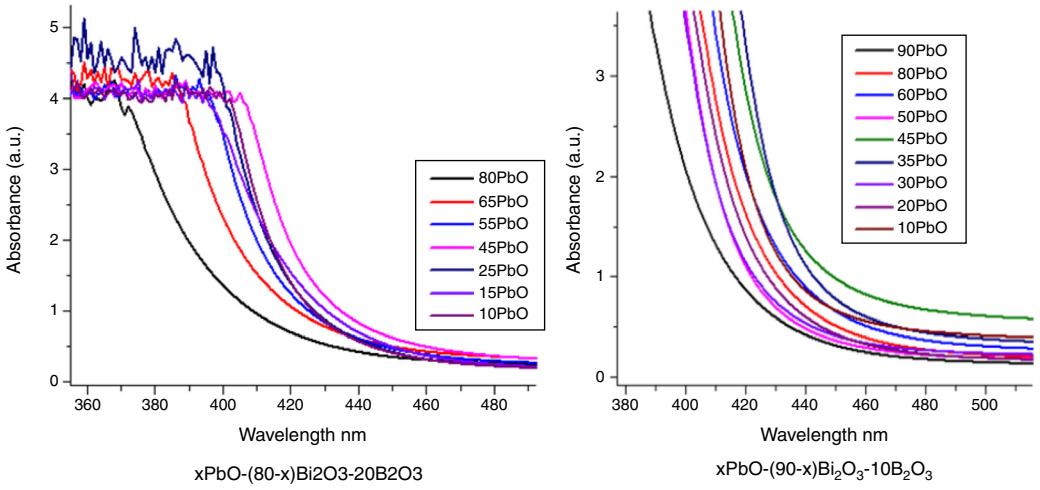

Fig. 9 – UV-vis spectra for obtained PBB glasses.

oxygen atom of PbO is used to convert two B_2O_3 units to two BO_4 units. For example, in glasses PBB16, PBB17, PBB26, PBB27 and PBB29, PbO entered the glass network by breaking up the Bi\O\Bi and B\O\B bonds and introduced coordinate defects known as dangling bonds along with non-bridging oxygen ions (Bi\O\...Pb^{2+}...\O\Bi), which in turn neutralize the negative charge of non-bridging oxygen ions by forming BiO_6 and BO_4 units [26]. Therefore, Pb^{2+} acted as a glass forming agent and was incorporated in the form of PbO_4 units [32].

Pb^{2+} fulfills a dual role in glass structure depending on its concentration. With the PbO content increased, a considerable portion acted as a double bridge between adjacent Bi_2O_3 and form –Bi\O\Pb\O\Bi – besides PbO_4 and BiO_3 units. As can be seen from the structure of PbO in Fig. 3, Pb^{2+} ions are likely to form compact pyramidal PbO_2 units. These pyramidal units reduce the availability of ionic charge balance, and reduce the formation rate of tetrahedral [BO_4] units. As for Bi_2O_3, due to their high polarizability and asymmetric octahedra [BiO_6], Bi^{3+} in glass may exist in six and eight-coordination [10].

The IR spectra of pure B_2O_3 gives two absorption band at wave-numbers 1300–1700 and 720 cm^{-1}, but from Fig. 11, the frequency from 500 to 1500 cm^{-1} is linear. This is due to the low B_2O_3 content in these glasses in which B_2O_3 did not act as main network former. So the absorption band at 720 cm^{-1} was covered and cannot be observed. However, bands from 1500 cm^{-1} to 1700 cm^{-1} are attributed to the bending vibration and stretching vibration of B—O—B in [BO_3] triangles [44,45]. Glasses with 20% B_2O_3 content had higher intensity in these bands than glasses with 10% B_2O_3. In addition, with increase of HMO content, the frequency of [BO_4] unit in glass with 20% B_2O_3 shifted to a lower frequency (from 1500 cm^{-1} → 1450 cm^{-1}) (Fig. 2 onset). This was due to the formation of bridging bonds of Pb—O—B and Bi—O—B. Since the stretching force constant of Pb—O bonding is substantially lower than that of the B–O, with the increase of HMO content, the stretching frequency of Pb—O—B might tend to be lower, and Pb—O—B bonds became dominant in glass network. It can be presumed that the increasing polarization of Pb^{2+} and Bi^{3+} contributed to the formation of Pb—O—B rings and their chains [46].

From Fig. 11, HMO glasses had high transmission (up to more than 80%) in the far-infrared region. The transmissions of glasses with HMO 80% are higher than glass with 90% HMO

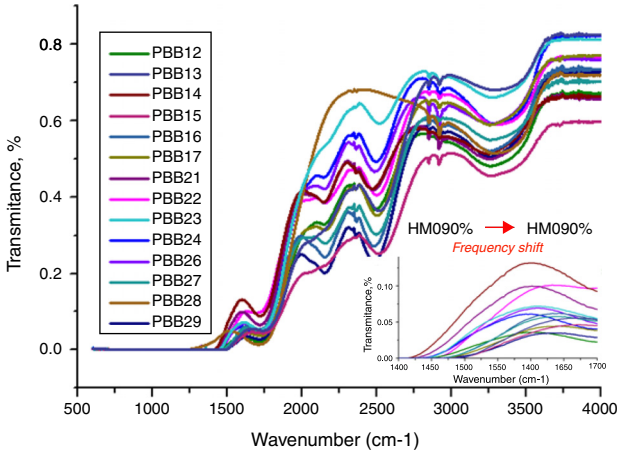

Fig. 10 – FT-IR spectra for PBB glasses with different compositions.

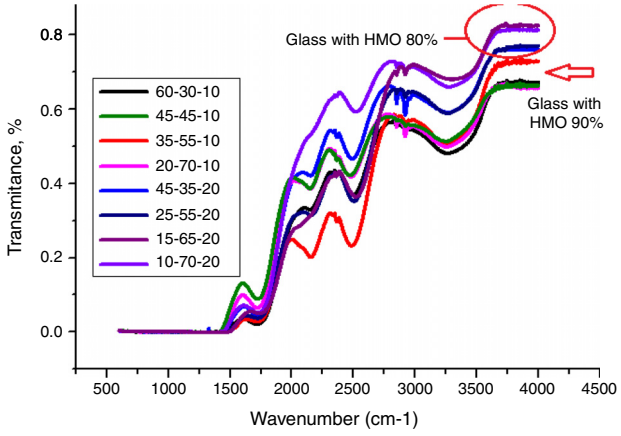

Fig. 11 – FT-IR spectra for PBB glasses with different compositions.

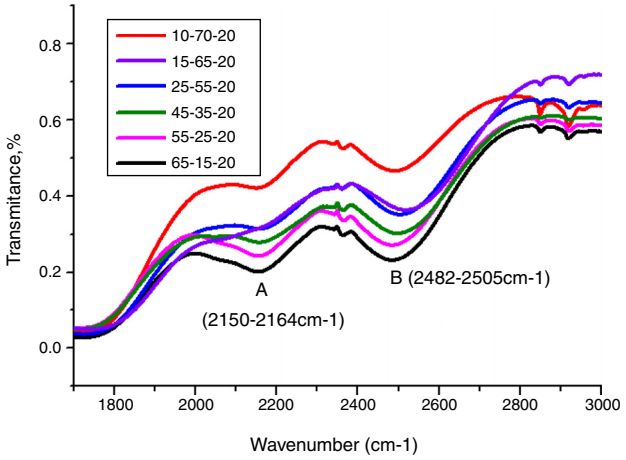

Fig. 12 – FT-IR spectra of PBB glasses with different compositions.

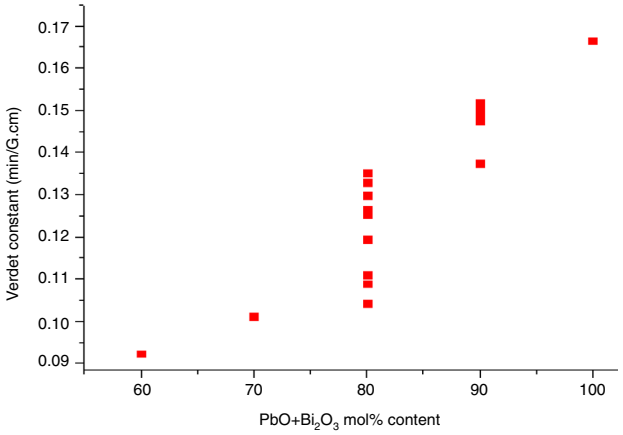

Fig. 13 – Verdet constant of PBB glasses with different compositions.

as shown in Fig. 12. PBB13 glass has the highest transmission (82.39%) in the range of 3500–4000 cm^{-1}. Peaks located around 3450 cm^{-1} are assigned to O—H absorption [45] because these glasses were fabricated in air.

Peaks around 2160 cm^{-1} (A) and 2500 cm^{-1} (B) in Fig. 12 are caused by the Pb—O bond vibration [29,46]. With increase PbO at the expense of Bi_2O_3, these two bands occurred obvious broader in shape and stronger in intensity which indicated the electrostatic fields of the strongly polarizing Pb^{2+} ions are enhanced by the vibration between Pb—O bonds.

Verdet constant and figure of merit

It is known that the Verdet constant of a magnetic–optical material is related to the electron shell structure of the atoms in glass. If the ions have the electron structure same with inert gas, the applied field can induce the Zeeman splitting on the ion energy levels. Basing on classical electromagnetism theory [19,32], Bacquerel has proposed the relationship between Verdet constant and diamagnetic properties of the materials in Eq. (1):

$$V_d = -\left(\frac{e}{2mc}\right)\lambda\frac{dn}{d\lambda} \quad (1)$$

where e and m are the charge and mass of the free electron, c is the light speed, $dn/d\lambda$ is the dispersion, V_d is the Verdet constant. From Eq. (1), the Verdet constant increased with the dispersion of the medium. In fact, the Pb^{2+}, Bi^{3+} ions exhibited high dispersion ability through the increase of non-bridging oxygen and structural distortion etc., so glasses with higher HMO content had higher Verdet constant as shown in Fig. 13.

On the other hand, the dispersion is proportional to the cation polarizability of glass [18], so the Verdet constant (V) can be expressed by the polarizability (α) in Eq. (2):

$$V = \frac{-3}{4}\frac{\alpha^2 I}{r^6} \quad (2)$$

where r is the distance between the atoms or molecules, I is the first ionization energy of atom and α is the polarizability constant expressed in units of m^3. The polarizability α represents the polarizability state of an average oxide cation in the glass matrix and its ability to attract electron density to surrounding ions. High oxide cation polarizability means strong electron attract ability of the oxide ion and vice versa. From Eq. (2), Verdet constant is proportional to the cation polarizability of glass. Substituting PbO with Bi_2O_3 in the borate glasses increases refractive index and dispersion [33]. Bi_2O_3 has bigger polarizability (1.508 $Å^3$) than PbO [47]. This is due to the fact that PbO offers only one atom per molecule, whereas Bi_2O_3 contributes two bismuth cations per molecule. Additionally, Bi^{3+} cation possesses an extremely low unit field strength which strongly affects the electron charge density of the surrounding oxygen ions. So Bi^{3+} cation has very high polarizability (1.508 $Å^3$) and a strongly polarized lone pair in the valence shell. These characteristics are responsible for the decrease of polarizing effect of these cations on the oxide ion and increase of non-oxygen bridge, and eventually contributed to the increase of Verdet constant. The Verdet constants for glasses with different Bi_2O_3 and PbO contents are shown in Fig. 14.

Basing on the quantum theory [19], Verdet constant of diamagnetic material is also related to the ion carriers with energy level splitting possibility (Eq. (3)):

$$V_d = (4\pi N\upsilon^2)\sum_n\left[\frac{A_n}{(\upsilon^2-\upsilon_n^2)^2}\right] \quad (3)$$

where V_d is the Verdet constant, N is the carriers in per unit volume, υ is the frequency of the incident wave, υ_n is the frequency of electrons migration, and A_n is the parameters correlative with migration intensity. Eq. (3) shows that the Verdet constant is related to the carriers' concentration N. In case of this study, the Pb^{2+} and Bi^{3+} ions are the carriers. Therefore glasses containing 90% HMO had higher Verdet constant than glasses with 80% HMO.

On the other hand, based on same HMO content, when substituting PbO with Bi_2O_3, the carriers per unit volume (or carriers' concentration) increases because PbO contributes only one Pb^{2+} per molecule, whereas Bi_2O_3 contributes two

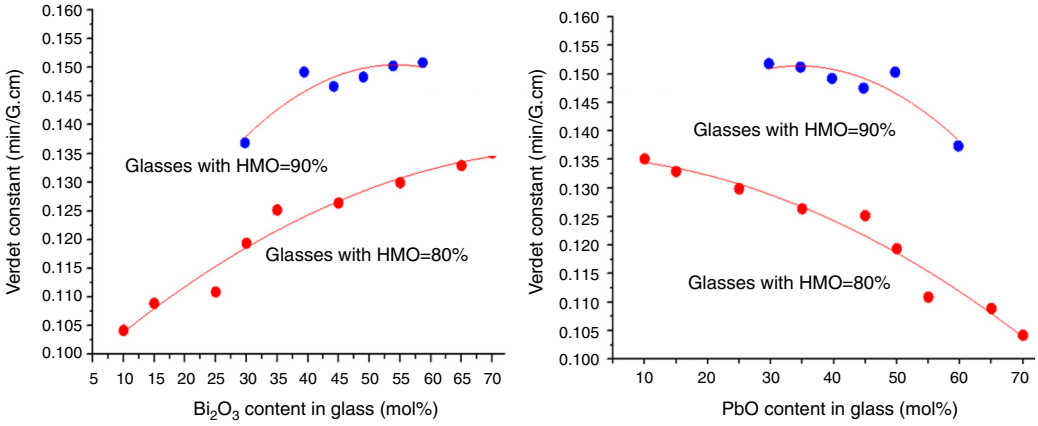

Fig. 14 – Verdet constant of glass with different HMO contents.

Bi^{3+}. Additionally, the electronic mass of Bi^{3+} is higher than Pb^{2+} but ionic radius of Bi^{3+} is smaller (1.20 Å) than Pb^{2+} (1.32 Å), these factors induce the decrease of molecule volume. Due to their more carriers' number, less molecule volume, higher carriers' concentration, Bi^{3+}-rich glasses exhibited higher Verdet constant than Pb^{2+}-rich glasses.

From Eqs. (1) and (3), it can be noticed that the Verdet constant depends on the incident wavelength (frequency). In this study, the Verdet constants of glass PBB13 were measured at three wavelengths (532 nm, 633 nm and 650 nm) as shown in Fig. 15.

It can be seen from Fig. 13, the Verdet constant decreased with the increasing of wavelength, and a fitting curve was made on base of the data, this agreed well with Eq. (1) and other reports on Verdet constants at different wavelengths [29].

Also from Eq. (3), the Verdet constant of a diamagnetic material has little temperature-dependence which makes PBB glass great advantageous over currently used crystal and paramagnetic counterparts. As addressed previously, the incorporation of HMO weaken the bridged O—B bonds and increase the non-oxygen bridge and induced an increase of structural disorder. So as a consequence the energy required for breaking down the glass network decreased (E_g) which leads to shift of cutoff to longer wavelength. Fig. 16 plots the Verdet constant of glasses with different cutoff wavelengths.

A fitting curve was normalized with the function of $V = -7.77544 + 0.03289\lambda - 3.38796E - 5\lambda^2$. It can be seen that the higher cutoff, the higher Verdet constant of glasses. The factors for example E_g, HMO content, cation polarizability, dispersion, electronic mass and radii etc., influenced both cutoff and Verdet constant of glass. From this study, it can be concluded that the increase of HMO content and the decrease of energy gap can improve the Verdet constant and cutoff redshift of glass. This conclusion agreed well with Ruan et al. [32] for chalcogenide glass.

Magneto-optical current sensor

The sensitivity of MOCT prototype based on glass with good thermal stability, high Verdet constant and high figure of merit was computed to be 8.31 nW/A, detailed descriptions about the calculation of sensitive can be found in [29].

Data of MOCT sensitivity has been plotted in Fig. 17. The X axis represents current flowing through the conductor ring, the Y axis represents signal intensity collected by the photodetector. Each measurement was repeated for 6 times, their

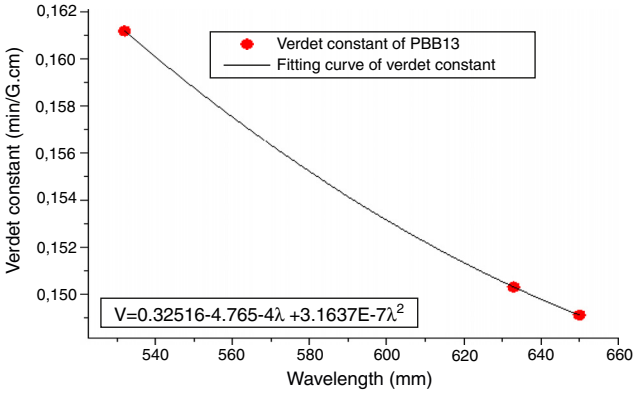

Fig. 15 – Normalized Verdet constant of glass PBB13 at three wavelengths.

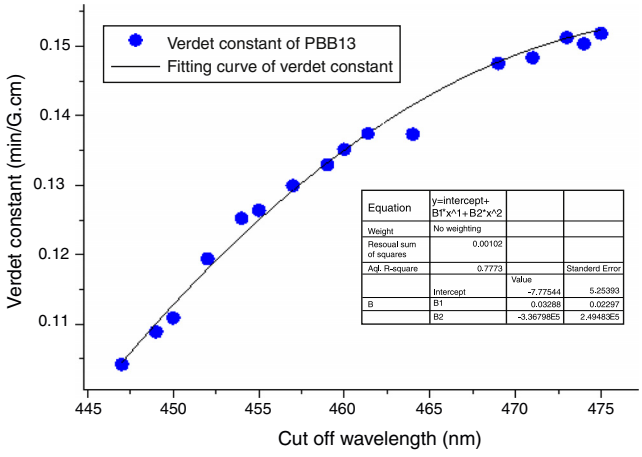

Fig. 16 – Verdet constant of PBB glasses with different cutoff wavelengths.

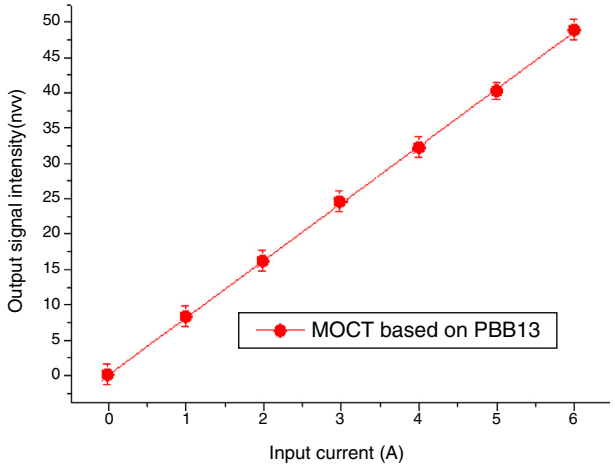

Fig. 17 – Linear response of MOCT prototype to applied different currents.

Table 3 – Comparison of sensitivity of this study and other OCTs.

	Sensing materials	Sensitivity (nW/A)
This study[a]	PBB13 glass	8.31
[29][a]	PBBGe glass	7.56
[48][a]	TZN glass	6.24
[49]	Bulk glass	0.072
[50]	Small bulk yttrium iron garnet	0.2
[5]	Flint glass SF2	13.75

[a] Study in this group.

mean value and their least mean squared curve-fit was computed. It is clear from the mean value that the response of the current sensor exhibits a high degree of current linearity. The fitting equation is: $I = 0.06429 + 8.902A$, the best fit is represented by a red line. The vertical error bars denote the uncertainties associated to each current measurement. From Fig. 17, one can confirm that good metrological properties of the constructed MOCTs were obtained.

Table 3 reports the sensitivity comparison of prototype in this study and optical current transducers (OCTs) from literature. Among influence factors, the material's Verdet constant (Faraday rotation effect) is the most important. From Table 3, it can be seen that even though the MOCT sensitivity based on PBB13 is smaller than flint SF2, it is still higher than PBBGe, TZN and others two glasses [49,50] based MOCT. The results proved ternary PBB glass has good potential for MOCT applications. Note that the sensitivity measurement is related laser power, sensing materials type, sample length and optical setup configuration etc. Which cannot be detailed from literatures, so Table 3 gives readers not a strict technical comparison on MOCT sensitivity.

Conclusion

Ternary PBB glasses with 80–90% HMO were prepared and characterized in terms of their glass forming ability, thermal stability, UV-vis spectra, FT-IR spectra and magneto-optical effects. Through the investigation on substitution of PbO with Bi_2O_3, it is found that PbO-rich glasses had a bigger glass forming range and better thermal stability than Bi_2O_3-rich glasses, Bi_2O_3 has substantial influence on glass devitrification. However due to its higher cation polarizability, Bi_2O_3 contributed much more to high refractive index, high Verdet constant and cutoff red-shift than PbO. The role of B_2O_3 depends on concentration. Among fabricated glasses, PBB13 exhibited the best thermal, magneto-optical performance and was applied on MOCT. High MOCT sensitivity proved the ternary PBB glasses are ideal candidate for magneto-optical devices.

Acknowledgement

Thanks to the National Natural Science Foundation of China NSFC (No. 61428502<tel:61428502>)

"studies on hybrid magneto-optic waveguide constructed with Fe:TiO2-SiO2 film on glass waveguide chips".

REFERENCES

[1] A.C.S. Brigida, I.M. Nascimento, S. Mendonca, J.C.W.A. Costa, M.A.G. Martinez, J.M. Baptista, Experimental and theoretical analysis of an optical current sensor for high power systems, Photon. Sens. 3 (1) (2013) 26–34.

[2] M.S. Ricardo, H. Martins, I. Nascimento, J.M. Baptista, A.L. Ribeiro, J.L. Santos, P. Jorge, O. Frazão, Optical current sensors for high power systems: a review, Appl. Sci. 2 (2012) 602–628.

[3] S.C. Rashleigh, R. Ulrich, Magneto-optic current sensing with birefringent fibres, Appl. Phys. Lett. 34 (1979) 768–770.

[4] P.R. Watekar, Ju S. Kim, S. Jeong, Y. Kim, W.T. Han, Development of a highly sensitive compact sized optical fiber current sensor, Opt. Express 18 (2010) 17096–17105.

[5] J. Zubia, L. Casado, G. Aldabaldetreku, A. Montero, E. Zubia, G. Durana, Design and development of a low-cost optical current sensor, Sensors 13 (2013) 13584–13595.

[6] E.P. Golis, A. Ingram, Investigations of magneto-optic properties in $PbO–Bi_2O_3–GeO_2$ glass system, J. Phys. Conference Series 79 (2007) 012003.

[7] Y. Cheng, H. Xiao, Structure and crystallization kinetics of $PbO–B_2O_3$ glasses, Ceram. Int. 33 (2007) 1341–1347.

[8] G.E. Rachkovskaya1, G.B. Zakharevich, Properties, structure, and application of low lead-bismuth glasses, Glass Ceram. 61 (2004) 9–12.

[9] B.N. Meera, J. Ramakrishna, Raman spectral studies of borate glasses, J. Non-Cryst. Solids 159 (1993) 1–21.

[10] L.R.P. Kassab, L.C. Courrol, $GeO_2–PbO–Bi_2O_3$ glasses doped with Yb^{3+} for laser application, J. Non-Cryst. Solids 348 (2004) 103–107.

[11] Q. Chen, M. Ferraris, D. Milanese, et al., Novel Er-doped PbO and B_2O_3 based glasses: investigation of quantum efficiency and non-radiative transition probability for 1.5 μm broadband emission fluorescence, J. Non-Cryst. Solids 324 (1–2) (2003) 12–20.

[12] Y.R. Rao, K.K. Goud, E.R. Kumar, M.C. Reddy, B.A. Rao, Upconversion luminescence in Er^{3+}/Yb^{3+} codoped lead bismuth indium borate glasses, Int. J. Recent Dev. Eng. Technol. 3 (2014) 122–130.

[13] Y.R. Rao, K.K. Goud, B.A. Rao, Luminescence studies of $PbO–Bi_2O_3–Ga_2O_3–B_2O_3$ glasses doped with Er^{3+}/Yb^{3+}, AIP Conf. Proc. 1536 (2013) 661–662.

[14] S.P. Singha, R.P.S. Chakradhara, J.L. Raob, B. Karmakara, EPR, FTIR, optical absorption and photoluminescence studies of Fe_2O_3 and CeO_2 doped $ZnO–Bi_2O_3–B_2O_3$ glasses, J. Alloys Compd. 493 (2010) 256–262.
[15] H. Yin, G. Zhao, P. Liu, S. Wang, H. Guo, Preparation and performance of magneto-optical glasses doped with $Tb^{3+/}Dy^{3+}$, Adv. Mater. 29 (2014) 684–687.
[16] P.V. Rao, M.S. Reddy, V.R. Kumar, Y. Gandhi, N. Veeraiah, Dielectric dispersion in $PbO–Bi_2O_3–B_2O_3$ glasses mixed with TiO_2, Turk J. Phys. 32 (2008) 341–356.
[17] D. Lezal, J. Pedlikova, P. Kostka, Heavy metal oxides glass: preparation and physical properties, J. Non-Cryst. Solids 284 (2001) 288–295.
[18] R.N. Brown, Material dispersion in heavy metal oxide glasses containing Bi_2O_3, J. Non-Cryst. Solids 92 (1987) 89–94.
[19] C.B. Pedroso, E. Munin, A.B. Villaverde, Magneto-optical rotation of heavy-metal oxide glasses, J. Non-Cryst. Solids 231 (1998) 134–142.
[20] M. Ehasanulla, K. Srikanth, A.V. Rao, K.A. Emmanuel, Spectroscopic & magnetic properties of $PbO–Bi_2O_3–B_2O_3$ glasses doped with FeO, Rasayan J. Chem. 4 (2011) 343–353.
[21] Q. Chen, H. Wang, S. Perero, Q. Wang, Q. Chen, Structural, optical and magnetic properties of Fe_3O_4 sputtered $TeO_2–PbO–B_2O_3$ and $PbO–Bi_2O_3–B_2O_3$ glasses for sensing applications, J. Non-Cryst. Solids 408 (2015) 43–50.
[22] Q. Chen, H. Wang, Q. Wang, Q. Chen, Properties of tellurite core/cladding glasses for magneto-optical fibers, J. Non-Cryst. Solids 400 (2014) 51–57.
[23] V. Simon, O. Ponta, S. Simon, M. Neumann, Atomic environment changes induced by rare earths addition to heavy metal glasses, J. Optoelectron. Adv. Mater. 10 (2008) 2325–2327.
[24] N.M. Sammesa, G. Tompsetta, R. Phillips, C. Carson, A.M. Cartnerb, Characterisation and stability of the fast ion conductor $(Bi_2O_3)_{1-x}(pbO)_x$, Solid State Ionics 86–88 (1996) 125–130.
[25] N. Singh, K.J. Singh, K. Singh, H. Singh, Comparative study of lead borate and bismuth lead borate glass systems as gamma-radiation shielding materials, Nucl. Instrum. Meth. Phys. Res. B 225 (2004) 305–309.
[26] W.H. Dumbaugh, Heavy metal oxide glasses containing Bi_2O_3, Phys. Chem. Glasses 27 (1986) 119–123.
[27] H. Ahmadi Moghaddam, Preparation of ultra dispersive glasses for designing novel coatings, Prog. Color Color. Coat. 2 (2009) 7–21.
[28] Q. Chen, Q. Chen, S. Wang, A new Faraday rotation measurement method for the study on magneto optical property of $PbO–Bi_2O_3–B_2O_3$ glasses for current sensor applications, Open J. Inorg. Non-metal. Mater. 1 (2011) 1–7.
[29] Q. Chen, Q. Ma, H. Wang, Q. Chen, Structural and properties of heavy metal oxide Faraday glass for optical current transducer, J. Non-Cryst. Solids 429 (2015) 13–19.
[30] Q. Chen, Q. Chen, M. Ferraris, Effect of ceramic crucibles on magneto-optical $PbO–Bi_2O_3–B_2O_3$ glasses properties, New J. Glass Ceram. (2012) 41–50.
[31] C.W. Morey, The property of glass, in: Am. Chem. Soc., Monograph Series, Reinhold Publishing Corporation, 1954.
[32] Y. Ruan, R.A. Jarvis, et al., Wavelength dispersion of Verdet constants in chalcogenide glasses for magneto-optical waveguide devices, Opt. Commun. 252 (2005) 39–45.
[33] C.Z. Tan, J. Arndt, Faraday effect in silica glasses, Physica B: Condens. Matter 233 (1997) 1–7.
[34] R.K. Brow, Glass structure (1), in: Structural Theories of Glass Formation, Shelby, 1932 (Chapter 5).
[35] Y. Zhou, Y. Yang, Characterization of new tellurite glasses and crystalline phases in the $TeO_2–PbO–Bi_2O_3–B_2O_3$ system, J. Non-Cryst. Solids 386 (2014) 90–94.
[36] C. Gautam, A.K. Yadav, A.K. Singh, A review on infrared spectroscopy of borate glasses with effects of different additives, ISRN Ceram. 428497 (2012) 1–17.
[37] C.L. Babcock, Silicate Glass Technology Method, Wiley-Interscience, 1977.
[38] I. Fenderlik, Optical Property of Glass, Elsevier, 1983.
[39] M. Hamezan, H. Sidek, A. Zaidan, K. Kaida, A. Zainal, Elastic constants and thermal properties of lead-bismuth borate glasses, J. Appl. Sci. 6 (2006) 943–949.
[40] I. Fanderlik, Optical Properties of Glass, Elsevier, Amsterdam, 1983.
[41] A. Pan, A. Ghosh, A new family of lead bismuthate glass with a large transmitting window, J. Non-Cryst. Solids 271 (2000) 157–161.
[42] S. Lakshimi, S. Rao, G. Ramadevudu, Optical properties of alkaline earth borate glasses, Int. J. Eng. Sci. Technol. 4 (2012) 25–35.
[43] B. Appa Rao, Y. Raja Rao, Upconversion luminescence in Er^{3+}/Yb^{3+} codoped $PbO–Bi_2O_3–Al_2O_3–B_2O_3$ glasses, Mater. Sci. Eng. 73 (2015) 012095.
[44] Y. Cheng, H. Xiao, W. Guo, W. Guo, Structure and crystallization kinetics of $PbO–B_2O_3$ glasses, Ceram. Int. 33 (2007) 1341–1347.
[45] E.I. Kamitsos, A.P. Patsis, M.A. Karakassides, G.D. Chryssikos, Infrared reflectance spectra of lithium borate glasses, J. Non-Cryst. Solids 126 (1990) 52–67.
[46] L. Balachander, G. Ramadevudu, M. Shareefuddin, IR analysis of borate glasses containing three alkali oxides, Science Asia 39 (2013) 278–283.
[47] K. Barczak, Optical fibre current sensor for electrical power engineering, Techn. Sci. 59 (2011) 409–414.
[48] Q. Chen, Q. Ma, H. Wang, Q. Chen, Diamagnetic tellurite glass and fiber based magneto-optical current transducer, Appl. Opt. 54 (29) (2015) 8864–8869.
[49] B. Yi, B.C.B. Chu, K.S. Chiang, Magneto-optical electric-current sensor with enhanced sensitivity, Meas. Sci. Technol. 13 (2002) N61–N68.
[50] T. Yoshino, K. Minegishi, M. Nitta, A very sensitive Faraday effect current sensor using a YIG/ring-core transformer in a transverse configuration, Meas. Sci. Technol. 12 (2014) 317–320.